

Article

Theory of AdaDelSPGD Algorithm in Fiber Laser-Phased Array Multiplex Communication Systems

Jiayu Chen ^{1,2}, Jinsheng Liu ³, Long Han ⁴, Mingru Ci ⁴, Dongbo Che ^{1,2}, Lihong Guo ^{1,*} and Hongjun Yu ^{1,*}

¹ Changchun Institute of Optics, Fine Mechanics and Physics, Chinese Academy of Sciences, Changchun 130033, China; cjylian@mail.ustc.edu.cn (J.C.); chedb839@163.com (D.C.)

² Center of Materials Science and Optoelectronics Engineering, University of Chinese Academy of Sciences, Beijing 100049, China

³ The Northern Institute of Electronic Equipment of China, Beijing 100191, China; 13810897732@163.com

⁴ College of Optoelectronics Engineering, Changchun University of Science and Technology, Changchun 130022, China; 18004427279@163.com (L.H.); cimingru666@163.com (M.C.)

* Correspondence: guolh@ciomp.ac.cn (L.G.); 13634404920@139.com (H.Y.); Tel.: +86-136-3440-4920 (H.Y.)

Abstract: Stochastic parallel gradient descent (SPGD) algorithm is one of the most promising methods for effective coherent beam combination. However, the algorithm also has some disadvantages, such as slow convergence speed and local extremum. This paper proposes an AdaDelSPGD algorithm, which combines an AdaDelta algorithm with a SPGD algorithm, and improves the traditional AdaDelta algorithm with adaptive gain coefficient. It is worth noting that the adaptive gain coefficient can be adjusted in real time to improve the convergence rate. The effectiveness of the proposed algorithm is verified by relevant simulation experiments, and the results show that the proposed algorithm can significantly improve the convergence speed. Following the experiments with the fiber laser-phased array multiplex communication system, we can draw the conclusion that the addition of communication modulation reduces the beam quality, and the higher the modulation frequency, the worse the beam quality. However, adding the SPGD algorithm can improve the beam quality. The AdaDelSPGD algorithm proposed in this paper can further improve the beam quality, and the bit error rate of communication is also decreased after testing. This provides a foundation for further research on the fiber laser-phased array multiplex communication system.

Keywords: SPGD algorithm; laser communication; phase lock; laser coherent synthesis



Citation: Chen, J.; Liu, J.; Han, L.; Ci, M.; Che, D.; Guo, L.; Yu, H. Theory of AdaDelSPGD Algorithm in Fiber Laser-Phased Array Multiplex Communication Systems. *Appl. Sci.* **2022**, *12*, 3009. <https://doi.org/10.3390/app12063009>

Academic Editor: Vadim Samarkin

Received: 10 November 2021

Accepted: 8 March 2022

Published: 16 March 2022

Publisher's Note: MDPI stays neutral with regard to jurisdictional claims in published maps and institutional affiliations.



Copyright: © 2022 by the authors. Licensee MDPI, Basel, Switzerland. This article is an open access article distributed under the terms and conditions of the Creative Commons Attribution (CC BY) license (<https://creativecommons.org/licenses/by/4.0/>).

1. Introduction

In recent years, due to their strong anti-interference ability and high confidentiality, lasers have shown good application prospects in free-space optical communication, optical detection and ranging (LIDAR), image projection, laser radar, optical storage, and other fields [1–3].

IPG Photonics uses cascade pumping to achieve a 10,000 W fiber laser output [4]. The literature shows that the output power of IPG Photonics' single-fiber single-mode fiber laser reaches 20 kW, and that of a multi-mode fiber laser reaches 50 kW [5,6]. With the development of high-power fiber lasers, many countries have shifted the research and development of tactical laser weapons to high-power fiber laser weapons. The Zeus laser mine-clearing system developed by SPATA, Raytheon's Naval Laser Weapon System (Laws), and the Prototype fiber laser weapon developed by Euromissile have all been approved by the military [7–9].

At present, the maximum output power of an individual single-mode continuous fiber laser can reach 20 kW, but this is far from the requirement for high-energy lasers in some industries and in national defense. Thus, the output power of an individual single-mode fiber laser is limited [10]. Dawson et al., from the Livermore National Laboratory in the United States, analyzed in detail the factors limiting the improvement of the output power

of fiber lasers. According to their calculations, the theoretical output power limit of a single-mode single-frequency fiber laser is approximately 1.86 kW, and the theoretical output power limit of a single-mode wide-spectrum fiber laser is approximately 36.6 kW [11].

Therefore, it is not feasible to obtain a laser output satisfying the tactical high-energy laser system requirements only through a single fiber laser [12]. Through coherent combination technology, the output power of laser beam combinations has improved significantly in the past 20 years, resulting in outstanding performance in terms of output power, beam quality, and overall efficiency of various devices based on laser combination [13,14].

The laser coherent synthesis method has successfully solved the nonlinear effect of single fiber output power and the limitation of thermal damage [15]. The key difficulty of laser coherent combination is to realize the in-phase output of the whole laser array. At present, there are two main solutions of phase locking technology: passive phase locking [16], and active phase locking [17].

Researchers at the Abbe Photonics Center, University of Jena, Germany, achieved a coherent synthetic output of a four-unit high-power femtosecond pulse fiber laser through active phase compensation [18]. The average/peak output power of the system was 530 W/1.8 GW, and the system synthesis efficiency was up to 93%. In 2018, the research team reported a four-channel ultra-fast fiber laser coherent synthesis system with an average output power of 3.5 kW [19]. This system is the ultrafast fiber laser coherent synthesis system with the largest average output power reported.

With the development of adaptive optics, researchers have developed several active phase control methods for multi-channel coherent synthesis. Heterodyne, multi-jitter, and the optimization algorithm are the most widely used active phase control techniques.

Jesse Anderegg et al. achieved coherent fiber laser synthesis with a total output power of 8 W in four units using the heterodyne method [20]. S. J. Augst et al., MIT, used two commercial 10 W ytterbium-doped fiber amplifiers to achieve a coherent synthetic output based on heterodyne [21]. The Lincoln Laboratory used heterodyne method to achieve 32-channel fiber laser phase-locking [22]. A coherent synthesis system based on heterodyne phase control requires a reference beam and an array of detectors with the same number of combined beams. The phase control modules of each beam in the coherent synthesis system work in parallel. This means that the heterodyne phase control system has a higher system control bandwidth and stability. However, the heterodyne method requires that the co-axis of the reference light and the signal light of each path must be strictly parallel and perpendicular to the detector array. As the amount of system bundling increases, the number of control modules increases correspondingly, which leads to an increase in the system's complexity and a deterioration in the system's stability.

Researchers at HRL Laboratories in the United States have achieved a 7-cell, 1-watt coherent synthetic output of fiber lasers using multi-dither active phase control techniques [23,24]. Angel Flores et al., US Air Force Research Laboratory, reported the coherent synthesis of 16 narrow line-width fiber lasers, with a total output power of 1.4 kW [25]. The Kirtland Air Force Research Laboratory implemented a nine-channel high power fiber laser phase-locked beam without reference beam using the multi-dithering method [26]. Meanwhile, Thales Research Technology Laboratory obtained coherent beam synthesis of 64 independent amplifying fibers by using four-wave shear interferometer [27]. Compared with the heterodyne method, the multi-dither method has no reference light. The structure of the system is simple and easy to implement. However, the phase noise frequency of the system increases with the increase in the number of beam combination elements. In order to effectively control the phase of each unit beam, the carrier frequency of the phase modulation part of the system must be increased. The bandwidth of the phase control system is higher than the noise frequency of the coherent synthesis system, which undoubtedly makes the design of the phase control demodulation circuit more complex.

Considering the complexity of the system and the control effect, the optimization algorithm has been widely used in adaptive optics. The more commonly used adaptive stochastic optimization algorithms are mountain climbing, genetic algorithm, simulated

annealing and stochastic parallel gradient descent (SPGD) [28,29]. By comparing the application of various optimization algorithms in coherent laser synthesis, the convergence speed of mountain climbing and genetic algorithm is too slow. The convergence speed of the simulated annealing algorithm is slightly lower than that of the SPGD algorithm. Meanwhile, the SPGD algorithm not only has a fast convergence speed, but also has a good tolerance in dealing with power fluctuations [30]. Therefore, the SPGD algorithm has been widely used in recent years.

Researchers at the University of Maryland in the United States achieved the coherent synthesis of a seven-unit milliwatt fiber laser using SPGD algorithm phase control technology [31]. C. X. Yu et al., Massachusetts Institute of Technology, USA, reported a 48-channel milliwatt-level coherent fiber laser synthesis scheme [32]. In 2011, researchers from the MIT Lincoln Experiment used the SPGD algorithm to control the phase of each unit beam, and realized the coherent synthetic output of eight channels of a 0.5 kW commercial fiber laser amplifier [33]. M. Vorontsov's team realized coherent beam synthesis of 21 channels at a distance of 7 km using SPGD algorithm [34,35]. Zou et al. used SPGD algorithm to achieve two km laser aiming [36]. Then they realized a large-scale fiber laser array over 2.1 km [37]. In addition, China's National University of Defense Technology (CNNDT) applied SPGD algorithm to achieve a coherent beam synthesis system of 60 fiber lasers [38]. In 2021, Zuo et al. implemented 19 laser-phased array using SPGD algorithm [39,40]. Then, in 2022, they use a new evaluation function to optimize the SPGD algorithm. Wang et al. used SPGD algorithm to realize the coherent synthesis of 64 elements in phased array [41].

Several modification techniques have been used to improve the convergence of SPGD algorithm. Vorontsov et al. proposed a decoupled stochastic parallel gradient descent algorithm with adaptive change gain coefficients. Compared with the traditional SPGD algorithm, this algorithm has a significant improvement in convergence speed and system stability. However, this optimization technique requires prior knowledge of the system's performance metrics, which limits the kinds of applications available. In order to make up for the shortcomings of this algorithm, our laboratory proposed an adaptive stochastic parallel gradient descent (AdaSPGD) optimization algorithm, based on performance index changes in previous practice [42]. Initially, adaptive gain coefficients were first added to the algorithm to compensate phase errors more quickly [43], but this required very complex calculations. Subsequently, it is applied to the adaptive gradient descent (AdaGrad) algorithm [44] and the problem of straight convexity in deep learning [45,46].

This paper presents an AdaDelSPGD algorithm which can change the adaptive gain coefficient. This algorithm improves the SPGD algorithm to improve the convergence speed of coherent synthesis.

Section 2 describes the basic principle of the SPGD algorithm in phase-locked system of fiber laser-phased array, and proposes an AdaDelSPGD algorithm. The convergence speed and convergence effect of the two algorithms in N-channel fiber laser-phased array system are illustrated in detail by simulation. In Section 3, we test the spot contrast and main lobe energy concentration of fiber laser-phased array multiplex communication system after adding two algorithms, and we describe the difference in the optical power value and bit error rate (BER) of the system before and after adding the AdaDelSPGD algorithm. Finally, conclusions are provided in Section 4.

2. Theoretical Analysis and Simulation of the Improved SPGD Algorithm

A structural diagram of the N-channel fiber laser-phased array multiplex communication system with the SPGD algorithm is presented in Figure 1. The system is mainly composed of four subsystems: laser transmitting, communication modulation, phase locking, and communication receiving.

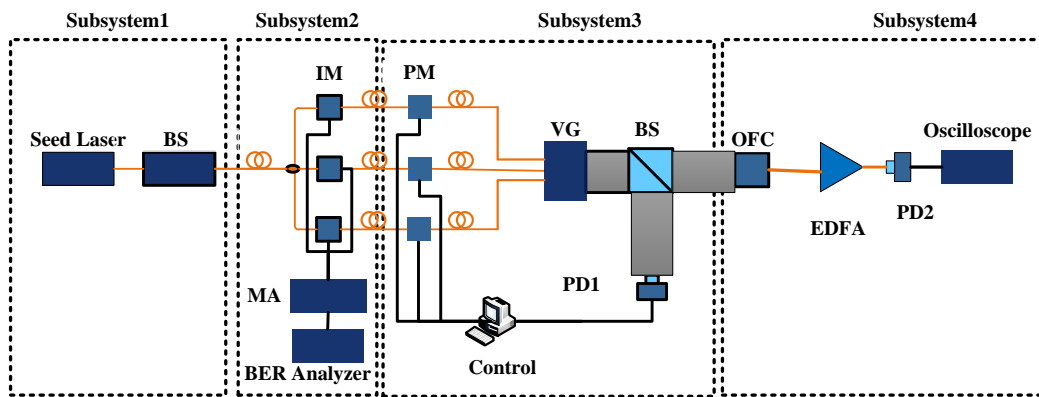


Figure 1. The scheme of the N-channel fiber laser-phased array multiplex communication system. MA: microwave amplifier; IM: intensity modulator; PM: phase modulator; VG: V-shaped groove; BS: beam splitting mirror; OFC: optical fiber collimator; PD1: Photo detector of phase locking; PD2: Photo detector of communication receiving system; EDFA: Erbium Doped Fiber Amplifier; Subsystem1: Laser transmitting system; Subsystem2: Communication modulation system; Subsystem3: Phase locking system; Subsystem4: Communication receiving system.

The laser transmitting subsystem is mainly composed of seed source and beam splitter, which is divided into N channels according to requirements.

The communication modulation subsystem mainly modulates the laser communication signal. The bit error rate analyzer and microwave amplifier provide the communication voltage signal. The signal is added to the N channel intensity modulator to conduct communication modulation of the laser.

The phase locking subsystem is a closed loop control system. After communication modulation, the optical signal goes through phase modulator first, and then through V slot beam output. The purpose of using V-groove here is to control the parallelism and spacing of N-channel laser. The laser output from the V-groove is then divided into two parts by a beam splitter. One part continues to output in this direction, while the other part enters the phase-locked detector (PD1). Here, an attenuator can be added before entering the detector according to the different power received by the detector. The voltage signal obtained by the detector enters the control module as a feedback signal. The algorithm is in the control module. After the algorithm, the new voltage value is added to the phase modulator.

The communication receiving subsystem is mainly used to receive the synthesized beam after communication modulation and phase lock, and analyze the laser through oscilloscope and detector. After the previous beam splitter, the laser is coupled to the optical fiber through the collimator, and then the optical signal is amplified by the optical fiber amplifier. Finally, the detector converts the optical signal into electrical signal and observes the effect of communication modulation through oscilloscope.

2.1. SPGD Algorithm and Simulation

The coherent combination process of n-channel fiber laser-phased array multiplex communication system using the traditional SPGD algorithm can be described by several steps. Firstly, the performance metric $J = J(u_1, u_2, \dots, u_N)$ is used as the algorithm's optimization object, which is a function of the phase control voltage $u = (u_1, u_2, \dots, u_N)$ of each sub-beam. Then, the phase controller applies a random microperturbation voltage satisfying Bernoulli distribution to each phase modulator. Unique extreme values are obtained by calculating changes $\delta J^{(n)} = J_+^{(n)} - J_-^{(n)}$ in performance indicators. The iteration formula of phase-controlled voltage update is:

$$u^{(n+1)} = u^{(n)} - \gamma \delta J^{(n)} u^{(n)} \quad (1)$$

where the superscript n is the number of iterations, and γ denotes the fixed gain coefficient of algorithm. When the performance index of the coherent synthesis system is optimized to the maximum, $\gamma < 0$; otherwise, $\gamma > 0$. If the fixed gain coefficient is too small and the iteration step is short, the convergence speed of the algorithm is slow, and it is difficult to realize real-time phase compensation. However, if the fixed gain coefficient is too large, the iteration step may cause the system performance evaluation function to fluctuate too much during the algorithm iteration, making the algorithm unstable.

In order to verify the effectiveness of SPGD algorithm in fiber laser-phased array multiplex communication systems, simulation analysis is carried out in free space environment. A 1064 nm laser beam with a waist of 5 mm was arranged in a honeycomb shape with an interval of 20 mm between each sub-beam. Using SPGD algorithm, PIB signal was used as the performance index of the system to control the phase of the transmitted beam. The initial phase value of the beam satisfied the Gaussian distribution between $[-\pi, +\pi]$ under zero mean value.

The performance measures obtained by SPGD algorithm in different gain systems (the average value of 100 independent runs) are shown in Figure 2. In addition, the convergences of the SPGD algorithm in three-channel and seven-channel laser coherent synthesis are shown in Figure 2a,b, respectively.

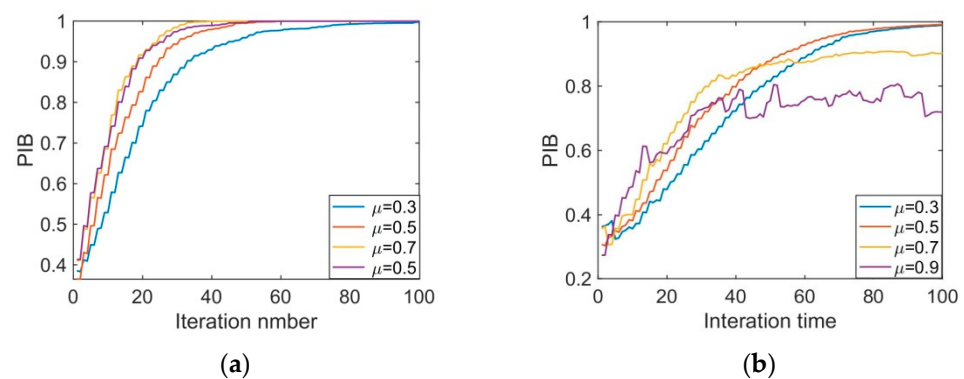


Figure 2. The relationship of system performance index with iteration times under different gain coefficients. (a) three-channel; (b) seven-channel.

As can be seen from the Figure 2, in the case of three-channel, the larger the iteration coefficient is, the faster the convergence rate is. But in the case of seven-channel, the expected value cannot be reached when the iteration coefficient is 0.9, so the iteration step size of the SPGD algorithm should not be too small or too large. If the step length is small, the speed is slow. If the step length of iteration is large, it may eventually fail to reach the maximum value of the target. Thus, we propose the AdaDelSPGD algorithm, hoping to improve the convergence speed and finally make the system stable at the target position at the same time.

2.2. AdaDelSPGD Algorithm and Simulation

The above algorithm is a conventional SPGD algorithm, and, based on the deep learning algorithm; this paper studies in detail the adaptive optimization of the SPGD iterative step size.

After the loss function is defined in deep learning, various methods are adopted to reduce the loss function. However, the value of the loss function is only a reference to optimize the parameters in the model. We optimized the loss function indirectly to optimize the model parameters and improve the measurement index of the model. Assuming that the objective function to be optimized is $J(\theta)$:

$$J(\theta) = E_{(x,y)\hat{p}_{data}} L(f(x, \theta), y) \quad (2)$$

where L is the loss function of every sample, $(f(x, \theta), y)$ is the input, x is the predicted output, y is the objective function, and \hat{p}_{dara} is the empirical distribution on the training set. However, theoretically, we hope that \hat{p}_{dara} is the real data distribution. In machine learning, empirical distribution is used to replace real distribution. Since not all sample data can be collected, only training sets are used for training. However, since the distribution of the data is not known, this machine learning problem is transformed into an optimization problem by finding the expectation and minimizing the expected loss. The purpose of optimization is to minimize the empirical risk:

$$E_{(x,y)\hat{p}_{dara}}L(f(x, \theta), y) = \frac{1}{m} \sum_{i=1}^m L\left(\left(f\left(x^i\right), \theta\right), y^\theta\right) \quad (3)$$

where m is the number of training samples. The training process based on this minimization of the mean training error is called experiential risk minimization.

In the training of deep learning, the number of samples in the training set is often tens of thousands, and the amount of computation required to traverse each sample to calculate the expectation is huge. In practice, a small amount of data is collected in the training set for calculation, and then the average value of these samples is calculated.

Stochastic gradient descent (SGD) is a classic optimization algorithm among small batch algorithms, which is often used in machine learning, especially in deep learning. Firstly, a small batch is generated by randomly selecting m samples from the training set, and then their gradient mean is calculated.

One disadvantage of the SGD method is that the update direction is completely dependent on the gradient calculated by the current subset, so it is very unstable. The momentum SGD algorithm borrows the concept of momentum in physics, which simulates the inertia of object motion; that is, the direction of the previous update is retained to some extent when updating, while the gradient of the current subset is used to fine-tune the final update direction. In this way, one can increase the stability to a certain extent, so that one can learn faster, and there is a certain ability to eliminate local optimality.

The previous series of optimization algorithms have a common feature; that is, each parameter is updated with the same learning rate. However, in practical application, the importance of each parameter is certainly different, so it is necessary to dynamically adopt different learning rates for different parameters, so that the objective function can converge faster.

The Adagrad algorithm is used to take the square of the gradient of each iteration of each parameter, add it and then square it, and divide the basic learning rate by this number, in order to perform the dynamic update of the learning rate. In this way, the learning rate of each parameter is related to its gradient, so the learning rate of each parameter is different, which is the so-called adaptive learning rate

The AdaDelta algorithm is an extension of the Adagrad algorithm. The original scheme is still an adaptive constraint on the learning rate, but it is simplified in calculation. The Adagrad algorithm will add up all the previous gradient squares, whereas the AdaDelta algorithm will add up only fixed-size terms (essentially the exponential moving average, using the average of the square of the previous steps), and will not store these terms directly, but only approximate the corresponding average (which is the advantage of the exponential moving average).

Based on the AdaDelta algorithm of deep learning, this study proposes the AdaDel-SPGD algorithm, which can adaptively change the iterative step size:

$$\begin{aligned} u_i^{n+1} &= u_i^n - \Delta\theta_k \delta J^n \delta u_i^n, i = 1, \dots, N \\ \Delta\theta_k &= \frac{\mu}{\sqrt{E[g^2]_k + \epsilon}} \end{aligned} \quad (4)$$

where the calculation formula of $E[g^2]_k$ is as follows, where ρ is 0.9:

$$E[g^2]_k = \rho E[g^2]_{k-1} + (1 - \rho)g_k^2 \tag{5}$$

The AdaDelSPGD algorithm we proposed for coherent fiber laser synthesis is described in detail as follows:

We firstly set the initial control voltage u_0 and the coefficient ρ . Generally, ρ is 0.9 in the experiment. Then, we will do a loop for finding the maximum value of the performance evaluation function $J(\cdot)$. The detailed steps are: (a) generating a set of randomly perturbed voltages that obey a Bernoulli distribution: $u = \{\delta u_i\}$; (b) applying a tiny forward perturbation voltage: $u + \delta u$; (c) obtaining performance evaluation functions: $J(u + \delta u)$; (d) applying a tiny negative perturbation voltage: $u - \delta u$; (e) obtaining performance evaluation functions: $J(u - \delta u)$; (f) obtaining the change of the evaluation function: $\delta J = J(u + \delta u) - J(u - \delta u)$; (g) updating $E[g^2]_k$ from the average of the previous expectation and the current gradient, $E[g^2]_k = \rho E[g^2]_{k-1} + (1 - \rho)g_k^2$; (h) updating gain coefficient: $\Delta\theta_k = \frac{\mu}{\sqrt{E[g^2]_k + \epsilon}}$; (i), obtaining the incremental control voltage: $u = u - \Delta\theta_k \delta J \delta u$. Finally, measuring the new performance evaluation function and judging whether the program satisfies the stop condition. If then stop condition has not been reached, repeating steps (a) to (i) until achieving the comfortable result.

Theoretically, the AdaDelSPGD algorithm improves the traditional SPGD algorithm in terms of gain factor. The adaptive gain coefficient improves the convergence rate of the coherent synthesis system. The following simulation clearly shows the change in convergence rate.

Under the same conditions as the SPGD algorithm, the AdaDelSPGD algorithm was simulated. The performance index of the AdaDelSPGD algorithm at different gain coefficients (average value of 100 independent operations) is shown in Figure 3. In addition, the convergence of the new algorithm is shown in Figure 3a,b when the coherent synthesis system is three-channel and seven-channel respectively.

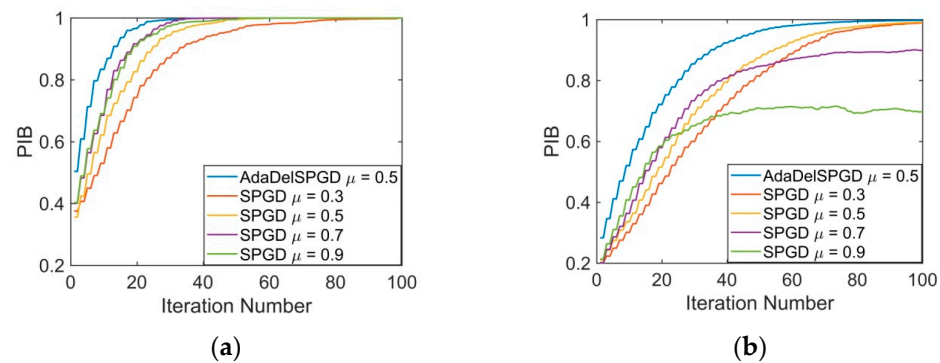


Figure 3. The changes in systematic performance with the number of iterations of two algorithms. (a) three-channel; (b) seven-channel.

Notably, the convergence speed of AdaDelSPGD algorithm is less affected by the gain coefficient than that of traditional SPGD algorithm. Since the adaptive gain coefficients weaken the influence of initial gain on the convergence of the algorithm, the optimal interval of the initial gain coefficients for different channels is almost constant (0.3–0.7). Therefore, the AdaDelSPGD algorithm can effectively eliminate the problem of improper selection of gain coefficients in practice.

Additionally, it can be observed that under the same number of channels, the convergence speed of the AdaDelSPGD algorithm is significantly faster than that of traditional SPGD algorithm. Taking the simulation results of the seven-channel system as an example, when the gain coefficient is too small, the convergence speed of the traditional SPGD algo-

rithm is too slow. At the same time, when the gain is too large, the traditional algorithm can not stabilize the phase-locked output.

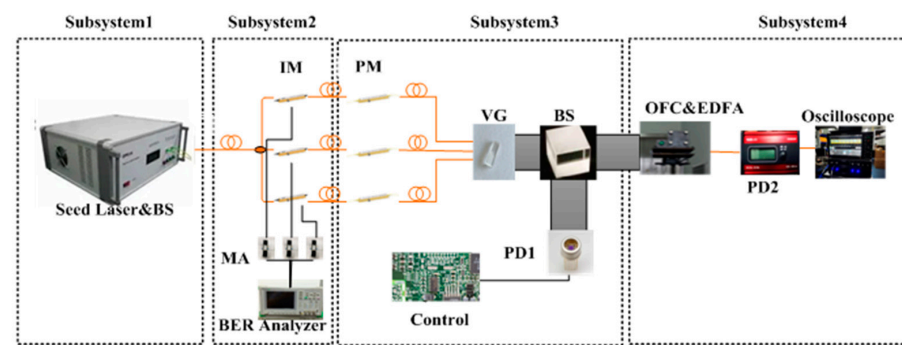
The relationship between the number of iterations required for convergence and the number of sub-beams of the two algorithms is presented in Table 1. The convergence speed of the AdaDelSPGD algorithm has improved by 38.4% and 44.4% for three-channel and seven-channel laser array systems, respectively. Therefore, the AdaDelSPGD algorithm can reduce the number of iterations, and the convergence effect is better than the traditional algorithm.

Table 1. The numerical results of the convergence speed.

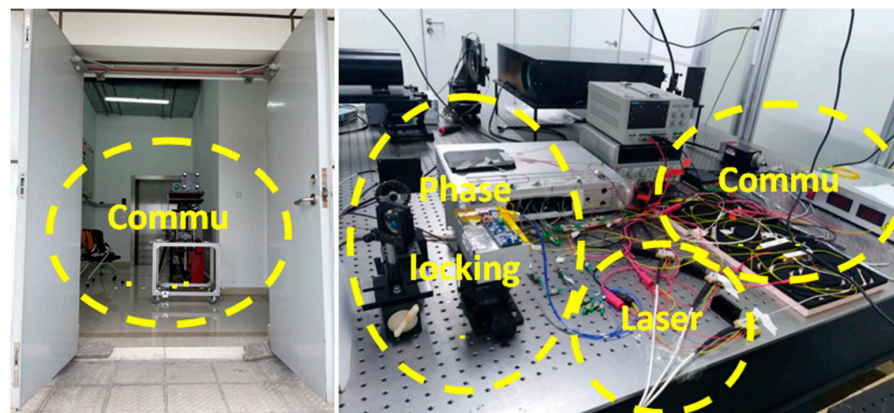
N	SPGD	AdaDelSPGD	Rate
3	18	13	38.4%
7	52	36	44.4%

3. Experiment

To verify the effectiveness of the algorithm, experiments are carried out in a three-channel fiber laser-phased array multichannel communication system. Figure 4a shows the experimental set-up, and Figure 4b shows the actual experiment. The experimental device is shown in Figure 4. For the convenience of display, the distance between PD and BS is reduced, while the actual distance is about 19 m, and the actual distance between BS and OFC is approximately 20 m or 3 km. The schematic diagram and the experimental process have been described in Section 2. Now, I will introduce the equipment used in the experiment used in each subsystem of the experiment in detail.



(a)



(b)

Figure 4. Diagram of the experimental device of the three-channel fiber laser-phased array multiplex communication system. (a) Set-up of the experiment; (b) experimental images.

In the laser emission subsystem, the seed source is a single-mode polarization-maintaining laser at 1064 nm, and the laser linewidth is less than 20 kHz. After passing through the inner part of the beam, the output power of the three laser channels is 1 mW.

The communication modulation subsystem adopts the bit error rate analyzer and microwave amplifier as the communication modulation signal input, and the intensity modulator is the ixBlue company's 10 GHz intensity modulator.

The phase modulator in the phase locking subsystem is an ixBlue phase modulator with a maximum modulation frequency of 150 MHz for a 1064 nm laser. The V-groove is custom made. The outer diameter of the optical fiber is 125 μm , and the distance between the centers of the three optical fibers is 127 μm after passing through the V-shaped groove. Therefore, the three optical fibers are closely arranged in the V-shaped groove. A spectroscopy transmits 90% of the light and reflects 10%. The detector is indium gallium as photodiode detector, with the maximum detection power of 10 mW. Since the three channels have a total of 3 mW, no attenuation film is used. The controller adopts DSP development board. The DSP algorithm control board algorithm processing core device is TMS320F2812 chip. The main frequency of the chip is 150 MHz. The A/D sampling module of the data acquisition part is AD976 chip, and the output D/A module uses two AD8544 chips.

In the communication receiving subsystem, there are four collimators altogether. Under laboratory conditions, only one collimator is coupled into the optical fiber. In the long-distance experiment, the compression divergence angle of the optical system was added to the emitter, but the diameter of the synthetic spot at 3 km was still 1 m. Therefore, four collimators are used to receive at the same time. Finally, when calculating the bit error rate, the four-bit error rates are averaged to increase the accuracy. The fiber amplifier model is YDFA-PA-MSA, and the detector is the THORLARS 'RXM25AF detector, with a frequency ranging from 500 kHz to 25 GHz. The oscilloscope model is Lecroy SDA813Zi. The bandwidth is 13 GHz. The eye chart and bit error rate were observed via oscilloscope.

3.1. Experiments on Different Communication Modulation Frequencies

When a continuous laser and a laser with different frequencies of communication signals were used as the light source, the experimental results of the three-channel fiber laser-phased array multiplex communication system were as presented in Figure 5. The interference fringes of the continuous laser are shown in Figure 5a; when the communication modulation frequency of each channel was 200 MHz and 500 MHz, respectively, the interference fringes were as shown in Figure 5b,c.

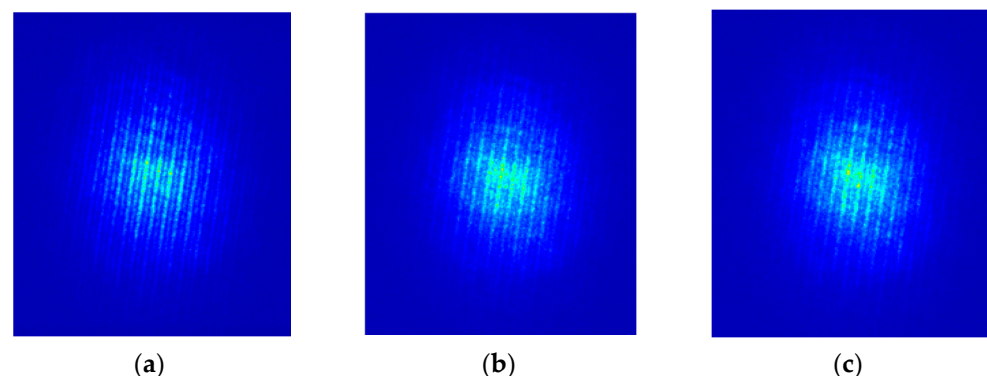


Figure 5. Images of interference fringes. (a) Continuous laser; (b) each way with 200 MHz communication; (c) each way with 500 MHz communication.

The streak contrast and main lobe energy concentration were selected as the evaluation criteria for interference fringe quality. (Streak contrast $V = (I_{\max} - I_{\min}) / (I_{\max} + I_{\min})$, in which I_{\max} is the maximum value of far-field beam intensity, and I_{\min} is the minimum value near the spot of I_{\max} .) The concentration of the main lobe energy was obtained by dividing

the sum of the energy of the main lobe by the sum of the energy of all the interference fringes after taking 10,000 points spaced equally by the interference pattern.

The streak contrast and main lobe energy concentration of interference fringes modulated by different communication modulation frequencies are shown in Table 2. It could be concluded that the beam quality decreased with the addition of the laser to the communication modulation, and the higher the frequency of communication modulation, the worse the beam quality.

Table 2. The beam quality of interference fringes.

	Continuous Laser	Each Way with 200 MHz Communication	Each Way with 500 MHz Communication
Streak contrast	0.566	0.454	0.356
Contrast reduction rate	-	19.8%	37.1%
Main lobe energy concentration	7.92%	7.15%	6.72%
Concentration reduction rate	-	9.7%	15.2%

3.2. Experiments Using Different Algorithms at the Same Communication Modulation Frequency

Next, the communication modulation frequency of the experimental variables was controlled consistently to verify the improvement effect of the different algorithms on beam quality. When the modulation frequency of each communication path was 500 MHz, Figure 6 presents the spot images obtained under different conditions without the algorithm, with the SPGD algorithm and with the AdaDelSPGD algorithm.

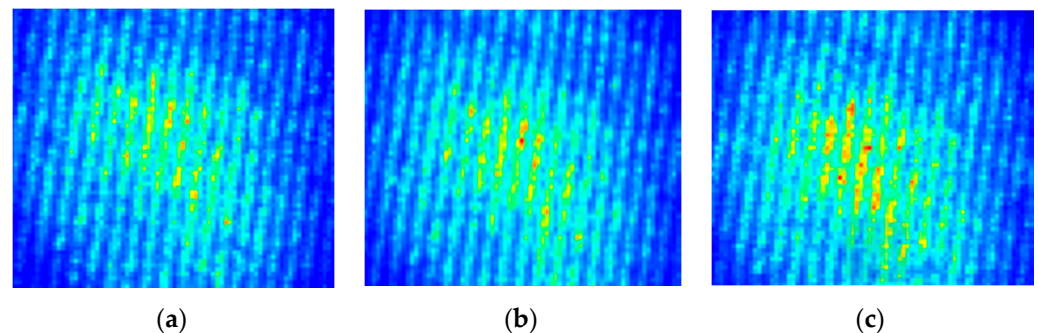


Figure 6. Images of interference fringes with 500 MHz communication each way. (a) Without algorithm; (b) with the SPGD algorithm; (c) with the AdaDelSPGD algorithm.

When the modulation frequency of each communication channel was 500 MHz, the calculated values of streak contrast and main lobe energy concentration were as shown in Table 3. It could be concluded that the SPGD algorithm could improve the streak contrast and main lobe energy concentration. The AdaDelSPGD algorithm proposed in this paper can further improve the beam quality under the same conditions; it can improve the contrast by 25.9%, and the main lobe energy concentration by 15.9%

Table 3. The beam quality of interference fringes of different algorithms.

	Without Algorithm	SPGD Algorithm	AdaDelSPGD Algorithm
Streak contrast	0.363	0.404	0.457
Contrast enhancement rate	-	11.3%	25.9%
Main lobe energy concentration	6.79%	7.18%	7.87%
Concentration enhancement rate	-	5.7%	15.9%

3.3. Experiments on the Influence of the Algorithm on the Bit Error Rate of Communication

The fiber laser-phased array communication system uses four channels of the same code to communicate at the same time, and each channel communication frequency is 8G. The purpose of multi-channel simultaneous communication is to increase the communication power and communication distance. Figure 7 shows the eye diagram of the experimental site.



Figure 7. The eye diagram of experimental site at 8G communication frequency.

The experiments were carried out in an indoor close-distance environment and an outdoor long-distance environment. If the distance between the receiving end and the transmitting end was 20 m, the transmitting power of each channel was 1 mW, for a total of 4 mW, and an optical fiber collimator was used to receive the data. The waveform before and after applying the AdaDelSPGD algorithm was observed by an oscilloscope. Optical power was measured using a detector, and the bit error rate was obtained by FPGA. When the distance between the receiving end and the transmitting end was 3 km, and the transmitting power of each channel was 20 W, for a total of 80 W. Due to the large size of the synthetic spot, four collimators were used to receive data, and the optical power and bit error rate were recorded. Multi-channel reception is conducive to improving the bit error rate. Before and after applying the AdaDelSPGD algorithm, the optical power values and BER values were obtained for both the inner and outer field experiments and are shown in Table 4. As can be seen from the table, the optical power was improved by more than 30%, and the bit error rate decreased before and after the AdaDelSPGD algorithm was added, regardless of the close indoor conditions or the long distance outside the city environment.

Table 4. The changes in optical power value and bit error rate before and after adding the AdaDelSPGD algorithm at different distances.

	20 m	3 km
The optical power value before algorithm	347 μ W	13 μ W
The optical power value after algorithm	471 μ W	17 μ W
Increase in optical power value	35.7%	30.8%
BER before algorithm	5.83×10^{-9}	7.64×10^{-6}
BER after algorithm	4.35×10^{-9}	5.90×10^{-6}

4. Conclusions

In this paper, the AdaDelSPGD algorithm is proposed, which contains an adaptive gain adjustment coefficient to accelerate convergence. Firstly, the working principle of the phased array system based on the AdaDelSPGD algorithm is analyzed. The simulation results show that the AdaDelSPGD algorithm can significantly improve the convergence speed compared with the traditional SPGD algorithm.

Based on the fiber laser-phased array communication system, the beam quality under different communication frequencies is analyzed. It is found that the quality of the beam is reduced by communication, and the higher the communication frequency, the lower the quality of beam. Secondly, by comparing the traditional SPGD algorithm and the AdaDelSPGD algorithm, it is proven that the AdaDelSPGD algorithm has a better effect. When three-channel 500 M communication is used, the contrast is improved by 25.9% and the main lobe energy concentration is improved by 15.9%. Finally, the optical power value and bit error rate are measured before and after the application of the AdaDelSPGD algorithm in different environments. The experimental results show that, after the algorithm is implemented, the optical power value is increased by more than 30%. When the communication distance is 20 m, the bit error rate of the system is reduced from 5.83×10^{-9} to 4.35×10^{-9} after phase locking by the AdaDelSPGD algorithm. When the communication distance is 3 km, the bit error rate of the system is reduced from 7.46×10^{-6} to 5.90×10^{-6} after phase locking by the AdaDelSPGD algorithm.

Author Contributions: Conceptualization, H.Y., J.L. and L.G.; methodology, H.Y., J.C. and J.L.; software, J.C.; validation, H.Y. and J.C.; formal analysis, J.C.; investigation, H.Y., J.C. and J.L.; resources, J.L.; data curation, J.C., L.H. and M.C.; writing—review and editing, J.C. and D.C.; visualization, J.C., L.H. and M.C.; supervision, H.Y., J.L. and L.G.; project administration, H.Y., J.L. and L.G.; funding acquisition, H.Y. and J.L. All authors have read and agreed to the published version of the manuscript.

Funding: This research received no external funding.

Institutional Review Board Statement: The study did not require ethical approval. This study is not applicable to humans or animals.

Informed Consent Statement: Not applicable.

Data Availability Statement: Not applicable.

Conflicts of Interest: The authors declare no conflict of interest.

References

1. Booth, M.J. Adaptive optical microscopy: The ongoing quest for a perfect image. *Light Sci. Appl.* **2014**, *3*, e165. [[CrossRef](#)]
2. Bar-Noam, A.S.; Farah, N.; Shoham, S. Correction-free remotely scanned two-photon in vivo mouse retinal imaging. *Light Sci. Appl.* **2016**, *5*, e16007. [[CrossRef](#)] [[PubMed](#)]
3. Yan, Y.; Chao, G.; Feng, L.; Guan, H.; Li, X. Multi-aperture all-fiber active coherent beam combining for free-space optical communication receivers. *Opt. Express* **2017**, *25*, 27519.
4. Injeyan, H.; Goodno, G.; Palese, S. *High Power Laser Handbook*; McGraw-Hill: New York, NY, USA, 2011.
5. Hecht, J. Fiber lasers ramp up the power. *Laser Focus World* **2009**, *45*, 53–57.
6. Shiner, B. The impact of fiber laser technology on the world wide material processing market. In *CLEO: Applications and Technology*; Optical Society of America: San Francisco, CA, USA, 2013.
7. Pawlak, R.J. Recent developments and near term directions for navy laser weapons system (laws) testbed. *Proc. SPIE Int. Soc. Opt. Eng.* **2012**, *8547*, 854705.
8. Mohring, B.; Dietrich, S.; Tassini, L.; Protz, R.; Geidek, F.; Zoz, J. High-energy laser activities at MBDA Germany. In *SPIE Defense, Security, and Sensing*; International Society for Optics and Photonics: Baltimore, MD, USA, 2013.
9. Ludewigt, K.; Riesbeck, T.; Graf, A.; Jung, M. 50 kw laser weapon demonstrator of rheinmetall waffe munition. *Proc. SPIE Int. Soc. Opt. Eng.* **2013**, *8898*, 88980N.
10. Otto, H.; Jauregui, C.; Limpert, J.; Tünnermann, A. Average power limit of fiber-laser systems with nearly diffraction-limited beam quality. In *Fiber Lasers XIII: Technology, Systems, and Applications*; SPIE: Bellingham, WA, USA, 2016.
11. Dawson, J.W.; Messerly, M.J.; Heebner, J.E.; Pax, P.H.; Sridharan, A.K.; Bulington, A.L.; Beach, R.J.; Siders, C.W.; Barty, C.P.J.; Dubinskii, M. Power scaling analysis of fiber lasers and amplifiers based on non-silica materials. In *Proceedings of the SPIE Defense, Security, and Sensing*, Orlando, FL, USA, 5–9 April 2010; Volume 7686, p. 768611.

12. Zhu, J.; Zhou, P.; Wang, X.; Xu, X.; Liu, Z. Analysis of maximum extractable power of single-frequency Yb³⁺-doped phosphate fiber sources. *IEEE J. Quantum Electron.* **2012**, *48*, 480–484. [[CrossRef](#)]
13. Wang, H.; He, B.; Yang, Y.; Zhou, J.; Zhang, X.; Liang, Y.; Sun, Z.; Song, Y.; Wang, Y.; Zhang, Z. Beam quality improvement of coherent beam combining by gradient power distribution hexagonal tiled-aperture large laser array. *Opt. Eng.* **2019**, *58*, 066105.1–066105.6. [[CrossRef](#)]
14. Shi, W.; Fang, Q.; Zhu, X.; Norwood, R.A.; Peyghambarian, N. Fiber lasers and their applications [invited]. *Appl. Opt.* **2014**, *53*, 6554. [[CrossRef](#)]
15. Wei, X.; Jing, J.C.; Shen, Y.; Wang, L.V. Harnessing a multi-dimensional fibre laser using genetic wavefront shaping. *Light Sci.* **2020**, *9*, 149. [[CrossRef](#)] [[PubMed](#)]
16. Daniault, L.; Hanna, M.; Papadopoulos, D.N.; Zaouter, Y.; Mottay, E.; Druon, F.; Georges, P. Passive coherent beam combining of two femtosecond fiber chirped-pulse amplifiers. *Opt. Lett.* **2011**, *36*, 4023–4025. [[CrossRef](#)] [[PubMed](#)]
17. Huang, Z.; Tang, X.; Zhang, D.; Wang, X.; Li, J. Phase locking of slab laser amplifiers via square wave dithering algorithm. *Appl. Opt.* **2014**, *53*, 2163–2169. [[CrossRef](#)] [[PubMed](#)]
18. Klenke, A.; Breitkopf, S.; Kienel, M.; Gottschall, T.; Eidam, T.; Hädrich, S.; Rothhardt, J.; Limpert, J.; Tünnermann, A. 530 w, 13mj, four-channel coherently combined femtosecond fiber chirped-pulse amplification system. *Opt. Lett.* **2013**, *38*, 2283. [[CrossRef](#)] [[PubMed](#)]
19. Müller, M.; Klenke, A.; Steinkopff, A.; Stark, H.; Limpert, J. 35 kw coherently combined ultrafast fiber laser. *Opt. Lett.* **2018**, *43*, 6037. [[CrossRef](#)] [[PubMed](#)]
20. Anderegg, J.; Brosnan, S.; Komine, H.; Wickham, M. 8-w coherently phased 4-element fiber array. *Proc. SPIE Int. Soc. Opt. Eng.* **2003**, *4974*, 1–6.
21. Goodno, G.D.; Komine, H.; Mcnaught, S.J.; Weiss, S.B.; Redmond, S.; Long, W.; Simpson, R.; Cheung, E.C.; Howland, D.; Epp, P.; et al. Coherent combination of high-power, zigzag slab lasers. *Opt. Lett.* **2006**, *31*, 1247. [[CrossRef](#)] [[PubMed](#)]
22. Yu, C.; Kansky, J.; Shaw, S.; Murphy, D.; Higgs, C. Coherent beam combining of large number of pm fibres in 2-d fibre array. *Electron. Lett.* **2006**, *42*, 1024. [[CrossRef](#)]
23. Bruesselbach, H.; Minden, M.L.; Wang, S.; Jones, D.C.; Mangir, M.S. A coherent fiber-array-based laser link for atmospheric aberration mitigation and power scaling. *Proc. SPIE* **2004**, *5338*, 90–101.
24. Mangir, M.; Bruesselbach, H.; Minden, M.; Wang, S.; Jones, C. Atmospheric aberration mitigation and transmitter power scaling using a coherent fiber array. In Proceedings of the IEEE Aerospace Conference, Big Sky, MT, USA, 6–13 March 2004.
25. Sanchez, A.D.; Flores, A.; Shay, T.M.; Lu, C.A.; Robin, C. Coherent beam combining of fiber amplifiers in a kw regime. In Proceedings of the 2011 Conference on Lasers and Electro-Optics (CLEO), Baltimore, MD, USA, 1–6 May 2011.
26. Shay, T.M.; Benham, V.; Baker, J.T.; Sanchez, A.D.; Pilkington, S.D.; Lu, L.C. Selsynchronous and self-referenced coherent beam combination for large optical arrays. *IEEE* **2007**, *13*, 480–486.
27. Bourderionnet, J.; Bellanger, C.; Primot, J.; Brignon, A. Collective coherent phase combining of 64 fibers. *Opt. Express* **2011**, *19*, 17053–17058. [[CrossRef](#)] [[PubMed](#)]
28. Huang, G.; Lv, G.; Fan, Y.; Geng, C.; Li, X. Stable control of the fiber laser phased array under long-range turbulent atmosphere. *Opt. Laser Technol.* **2022**, *146*, 107528. [[CrossRef](#)]
29. Chang, H.; Su, R.; Long, J.; Chang, Q.; Ma, P.; Ma, Y.; Zhou, P. Distributed active phase-locking of an all-fiber structured laser array by a stochastic parallel gradient descent (SPGD) algorithm. *Opt. Express* **2022**, *30*, 1089–1098. [[CrossRef](#)] [[PubMed](#)]
30. Wang, X.; Zhou, P.; Ma, Y. High precision phase control system in coherent combining of fiber laser based on stochastic parallel gradient descent algorithm. *Acta Phys. Sin.* **2010**, *059*, 973–979. [[CrossRef](#)]
31. Ling, L.; Vorontsov, M.A. Phase-locking of tiled fiber array using spgd feedback controller. *Proc. SPIE Int. Soc. Opt. Eng.* **2005**, *5895*, 138–146.
32. Kansky, J.E.; Yu, C.X.; Murphy, D.V.; Shaw, S.E.J.; Lawrence, R.C.; Higgs, C. Beam control of a 2d polarization maintaining fiber optic phased array with high-fiber count. *Proc. SPIE Int. Soc. Opt. Eng.* **2006**, *6306*, 63060G.
33. Yu, C.X.; Augst, S.J.; Redmond, S.M.; Goldizen, K.C.; Murphy, D.V.; Sanchez, A.; Fan, T.Y. Coherent combining of a 4 kw, eight-element fiber amplifier array. *Opt. Lett.* **2011**, *36*, 2686–2688. [[CrossRef](#)] [[PubMed](#)]
34. Weyrauch, T.; Vorontsov, M.; Ovchinnikov, V.; Polnau, E.; Polnau, E.; Wu, G.; Ryan, T.; Maynard, M. Atmospheric turbulence compensation and coherent beam combining over a 7 km propagation path using a fiber-array system with 21 sub-apertures. In *Imaging and Applied Optics*; Optical Society of America: Seattle, WA, USA, 2014; p. PW2E.3.
35. Weyrauch, T.; Vorontsov, M.; Mangano, J.; Ovchinnikov, V.; Bricker, D.; Polnau, E.; Rostov, A. Deep turbulence effects mitigation with coherent combining of 21 laser beams over 7 km. *Opt. Lett.* **2016**, *41*, 840–843. [[CrossRef](#)] [[PubMed](#)]
36. Zou, F.; Zuo, J.; Geng, C.; Li, F.; Huang, G.; Liu, J.; Jiang, J.; Fan, Z.; Li, X. Adaptive Laser Aiming Through 2 km Horizontal Atmosphere with Precise-Delayed SPGD Algorithm. *J. Russ. Laser Res.* **2021**, *42*, 462–467. [[CrossRef](#)]
37. Zuo, J.; Zou, F.; Zhou, X.; Geng, C.; Li, F.; Jia, Q.; Jiang, J.; Li, Z.; Liu, J.; Ma, X.; et al. Coherent combining of a large-scale fiber laser array over 2.1 km in turbulence based on a beam conformal projection system. *Opt. Lett.* **2022**, *47*, 365–368. [[CrossRef](#)] [[PubMed](#)]
38. Su, R.; Zhou, P.; Wang, X.; Zhang, H.; Xu, X. Active coherent beam combining of a five-element, 800 w nanosecond fiber amplifier array. *Opt. Lett.* **2012**, *37*, 3978–3980. [[CrossRef](#)] [[PubMed](#)]
39. Zuo, J.; Li, F.; Geng, C.; Zhou, F.; Li, X. Experimental demonstration of central-lobe energy enhancement based on amplitude modulation of beamlets in 19 elements fiber laser phased array. *IEEE Photonics J.* **2021**, *13*, 1500113. [[CrossRef](#)]

40. Zuo, J.; Zou, F.; Geng, C.; Li, F.; Huang, G.; Liu, J.; Yang, X.; Jiang, J.; Fan, Z.; Ma, X.; et al. Experimental Demonstration of Efficient Coherent Combining of 19 Fiber Lasers By Adaptive Gain Coefficient SPGD Algorithm. *J. Russ. Laser Res.* **2021**, *42*, 609–617. [[CrossRef](#)]
41. Wang, X.; Liu, C.; Cao, Y.; Liu, R.; Zhang, L.; Zhao, X.; Lu, F.; Miao, Z.; Li, Q.; Han, X. High-precision two-dimensional beam steering with a 64-element optical fiber phased array. *Appl. Opt.* **2021**, *60*, 10002–10008. [[CrossRef](#)] [[PubMed](#)]
42. Song, J.; Li, Y.; Che, D.; Guo, J.; Wang, T. Coherent beam combining based on the spgd algorithm with a momentum term. *Optik* **2020**, *202*, 163650. [[CrossRef](#)]
43. Weyrauch, T.; Vorontsov, M.A.; Bifano, T.G.; Hammer, J.A.; Cohen, M.; Cauwenberghs, G. Microscale adaptive optics: Wave-front control with a μ -mirror array and a vlsi stochastic gradient descent controller. *Appl. Opt.* **2011**, *40*, 4243–4253. [[CrossRef](#)] [[PubMed](#)]
44. Duchi, J.; Hazan, E.; Singer, Y. Adaptive subgradient methods for online learning and stochastic optimization. *J. Mach. Learn. Res.* **2011**, *12*, 257–269.
45. Zhang, Y.C.; Kagen, A.C. Machine Learning Interface for Medical Image Analysis. *J. Digit. Imaging* **2017**, *30*, 615–621. [[CrossRef](#)] [[PubMed](#)]
46. Zhang, N.; Lei, D.; Zhao, J. An improved adagrad gradient descent optimization algorithm. In Proceedings of the 2018 Chinese Automation Congress, Xi'an, China, 30 November–2 December 2018.